Computational optimisation of optical projection tomography for 3D image analysis
Tang, X.

Citation
Tang, X. (2020, June 10). *Computational optimisation of optical projection tomography for 3D image analysis*. Retrieved from https://hdl.handle.net/1887/106088

Cover Page

Universiteit Leiden

Author: Tang, X.
Title: Computational optimisation of optical projection tomography for 3D image analysis
Issue Date: 2020-06-10

Chapter 1

Introduction

Chapter summary

In this chapter, we focus on presenting the general idea of our research interest and topics. It starts with the importance of three-dimensional imaging techniques in biomedical research, providing a broad view of the selection of imaging instruments according to the research requirements. Subsequently, we introduce the three-dimensional imaging system used in our research, i.e. optical projection tomography, and thoroughly elaborate it from the imaging schema, experimental setup, imaging software and sample preparation. Beside the imaging aspects, the computational approaches of optical projection tomography are explained, including three-dimensional reconstruction, segmentation and quantification. Following, seven research questions are formulated from our research perspective.

1.1 Importance of three-dimensional imaging in biomedical research

Microscopes are our eyes for things beyond our sight. Therefore, in research this instrument is indispensable. The standard microscope was designed to produce a two-dimensional (2D) image of a sample that would otherwise remain unobservable by the eyes. In this manner, an intuitive representation of details and structures can be easily transformed to an image. In the life sciences the requirement for imaging is far beyond just a qualitative description. Quantitative approaches for measurements are required.

Advances in molecular genetics have enabled molecular imaging to visualize processes in cells, cell cultures, tissues, organs and organisms with a resolution from less than a micrometer to centimeters. These possibilities are making a tremendous impact on biology and medical research. Genetic engineering technologies such as in situ hybridization as well as fluorescence staining permit the qualitative, quantitative and localization analysis of protein and gene expression patterns in animals and plants.

With respect to cells and cell cultures, the application of genetic engineering to cells allows studying signaling processes in cells and mono-layer cell cultures. However, these mono-layer cell cultures may exhibit non-physiological behavior within their artificial planar environment. Hence, there is a trend from *in vitro* to *in vivo* experimentation and thus a trend of understanding biology at the level of the scale of tissue or whole organism. Imaging modalities need to support this trend [1], [2].

In order to understand spatial organization and gene expression, three-dimensional (3D) imaging is required. On the level of tissues and organisms this has been accomplished by making physical thin sections and producing a 3D image through reconstructing from these physical sections. This technique, referred to as invasive imaging, is laborious and sometimes complicates an understanding of the sample through artefacts that are introduced in the process of sample preparation and imaging.

In the past decades, studies on disease mechanisms and drug discovery have also benefited from the high-resolution fluorescence microscopy techniques such as confocal laser scanning microscopy (CLSM) or multiphoton laser scanning microscopy (MLSM), enabling the visualization of parts of the cell signaling network [3], [4]. The sample in 3D is scanned in a plan parallel fashion using the optics in a smart manner. This approach, of non-invasive imaging, works well with cellular mono layers and relatively thin samples, i.e. in the range of tens of micrometers to a millimeter. Samples that are larger and thicker are less suitable for this kind of approach, i.e. samples larger than 2 millimeters to one centimeter. As indicated, one approach for imaging would be an invasive technique like serial sectioning. However, there are other options.

Classical non-invasive *in vivo* imaging tools such as computed tomography (CT), magnetic resonance imaging (MRI), positron emission tomography (PET) or single-photon computed tomography (SPECT) provide a spatial resolution in the millimeter scale at organ-level in living specimens and patients. These imaging techniques make significant contribution especially for disease models of the central nervous system

(CNS), such as brain tumours, Alzheimer's disease, or multiple sclerosis.

In terms of biology and optical imaging an efficient non-invasive instrument for imaging biological tissue, organ and organism is optical projection tomography (OPT). In the recent years, cancer progression [5]–[7], drug discovery [8] and development studies such as skeleton, teeth and blood vessels have successfully used OPT imaging [9]–[12].

Figure 1.1 briefly summarizes the range of resolution at which imaging techniques in bio-medical research operates. It ranges from nanometers to centimeters with imaging scale from protein to whole organism. The white color shown between two different types of imaging indicates some overlapping in scale where both types are being applied, depending on the experimental setup and research requirement.

With respect to OPT imaging, signal acquired covers 2D information. For this device, 3D imaging is archived by rotating the samples over a full revolution (360°) and at each step capture an image. The collection of these images is known as the tomogram. From the tomogram a 3D image is reconstructed. This reconstruction process is a computational process and requires design of smart algorithms and efficient computation strategies. An example of such reconstruction algorithm is the filtered back projection (FBP) algorithm [13].

The research in this thesis focusses on the application of OPT in biomedical research. Therefore, it deals with design and implementation of algorithms and computational strategies to deal with data, i.e. images that are acquired with an OPT microscope.
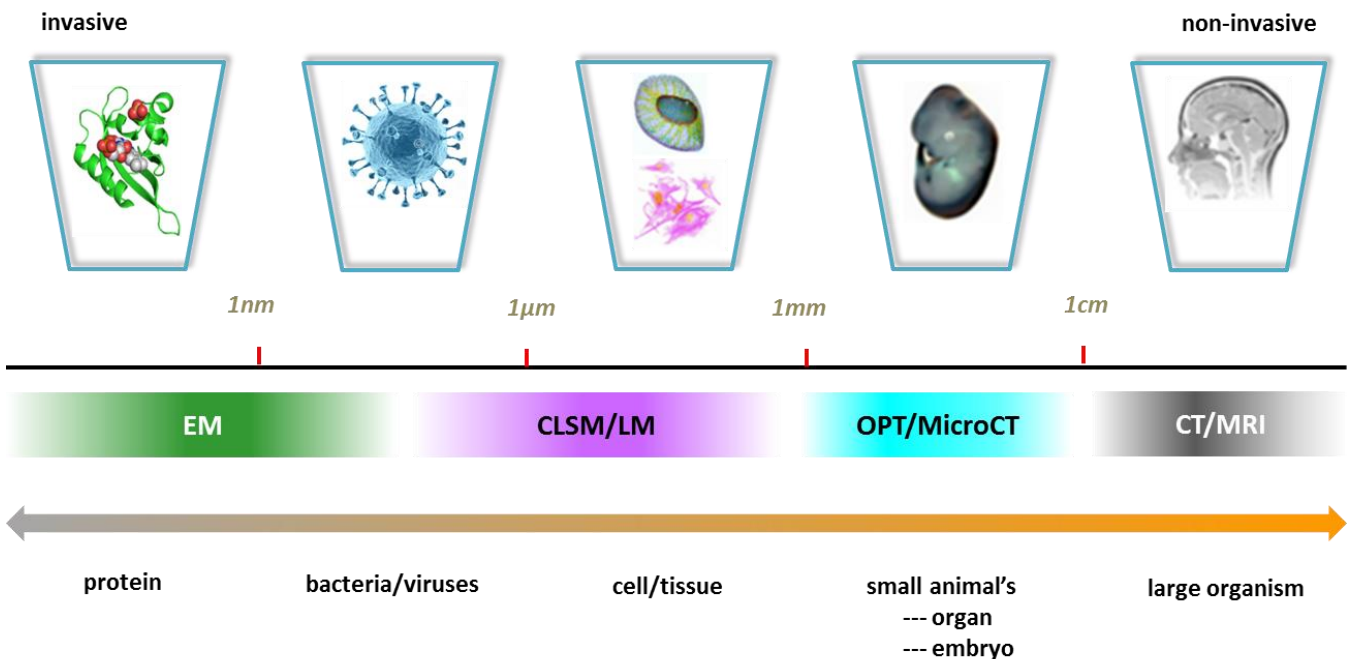

Figure 1.1. Overview of sample scale and the corresponding microscope applicable. The representations of different imaging levels are shown on the top from protein to organism, inspired by Alanis *et al.* [14].

1.2 Introduction of OPT imaging system

With respect to CLSM [15] we are confronted with a limitation of size of the specimen for whole-mount imaging. With MRI [16] the strength of the magnetic field determines the resolution that can be obtained for a whole-mount imaging. The OPT technique [17] for that matter, can overcome these shortcomings. It can visualize gene expression or specific staining in bright-field or fluorescence channel, while the specimen as a whole can be imaged. In that manner, OPT adds an important range of scale that can be imaged. It allows for the acquisition of high resolution full body images of animal/plant tissues as well as organs/organisms [18], [19]. It has been studied for the capability of imaging with good spatial resolution and contrast and minimal shadowing artefacts produced after reconstruction of a tomogram.

1.2.1 Introduction of OPT imaging schema

In Figure 1.2, we describe our imaging system conform the original set up as presented in [17]. We will focus on the OPT of zebrafish as this is the main specimen that we work with. The specimen is fixed for imaging in an agarose cylinder that can be rotated, mounted to a step motor unit using a magnet. Light transmitted (purple lines) is focused by the lenses onto the digital camera, i.e. Charge-Coupled Device (CCD). The apparatus is adjusted so that light emitted from a slice that is perpendicular to the rotation axis (red ellipse), is focused onto a single row of pixels on the CCD (red line). The slice highlighted as a red ellipse in (A) is seen as a red circle in (B). Different from CT imaging, in optical imaging system a pixel on the CCD contains the information of the specific slice of the specimen in the cone-shaped region (purple region). Points far from the focal plane will not be focused and will, as a consequence, not produce a sharp image. Contrarily, only the point closer to focal plane yields a high-quality image. The depth of the cone-shaped region is defined as depth of focus (DoF) which is determined by the property of lenses. For good OPT imaging the cone is ideally as narrow as possible and the DoF is expected to be large enough to include the whole specimen. But in practice, there is a trade-off between them; i.e, large DoF corresponds to wide cone. One typical way to solve this problem is to adjust the position of rotation centre so that only the front half of the specimen is in focus. This ensures that every part of the specimen is imaged in focus during a full revolution (360◦ rotation of the specimen). The sampled regions (C) from adjacent pixels are distributed across the section as an approximation of parallel line integrals.
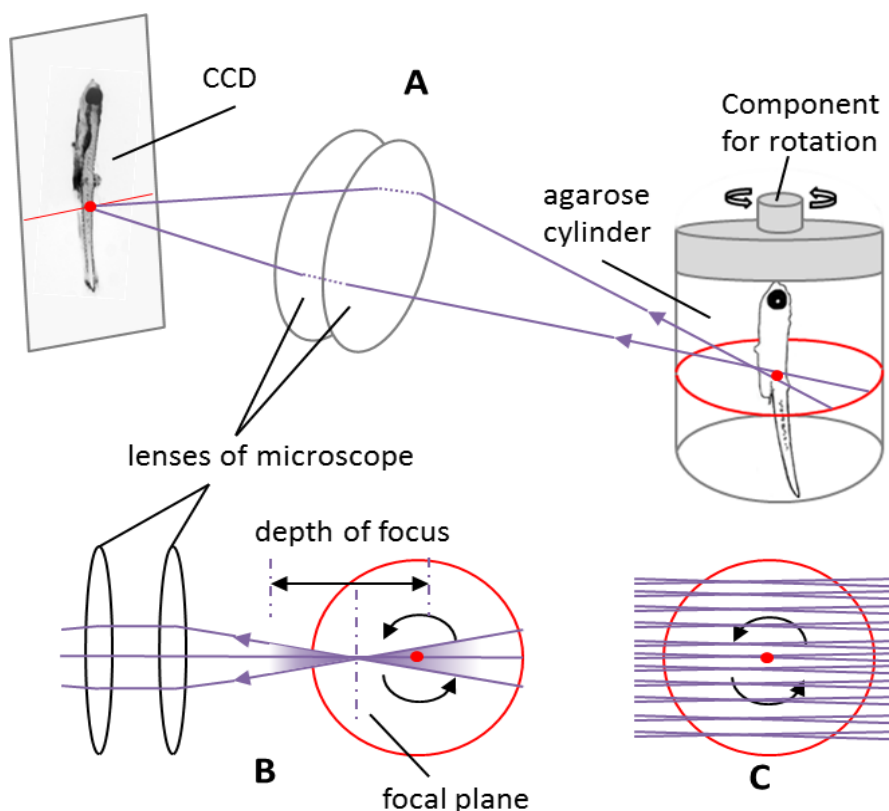
Figure 1.2. The schema of OPT microscopy imaging system. (A) The general imaging schema of a single pixel on a specific slice (red circle). (B) The optical explanation of a pixel of the image on CCD. (C) The formation of adjacent pixels of the image on a specific slice, i.e. the red line in (A).

1.2.2 Experimental OPT imaging setup

The flow diagram of our OPT imaging system is illustrated in Figure 1.3. It consists of a Leica MZ16 FA stereomicroscope with a Plan 0.5 and $135mm$ working distance objective lens (Leica 10446157). Images are acquired by a thermos electronically cooled Retiga Exi CCD camera with a chip size of 1036×1360. The images are saved as 16 bit tiff files but are effectively 12-bit from the Analog to Digital (AD) conversion. A full revolution of 400 images over 360◦ results in a 1.13Gb tiff-file. The acquisition is realized by a rotation of the specimen driven by a stepper unit, meaning that the stepper accomplishes a step of 0.9◦. The OPT imaging system has imaging modules: for the bright-field imaging, specimen is illuminated with a LED and for fluorescence imaging a 100W mercury lamp attached to the microscope housing is used in combination with a filter block. The optical path of the bright-field channel is shown in yellow while that of the fluorescence channel is illustrated in blue and green depending on configuration of the filter block for green fluorescent protein (GFP), e.g. as presented in Figure 1.3. In our imaging system there are three fluorescence channels available including GFP, YFP and TRX. The switch between the bright-field and fluorescence module is controlled by software through an Arduino controller that is integrated in the system.
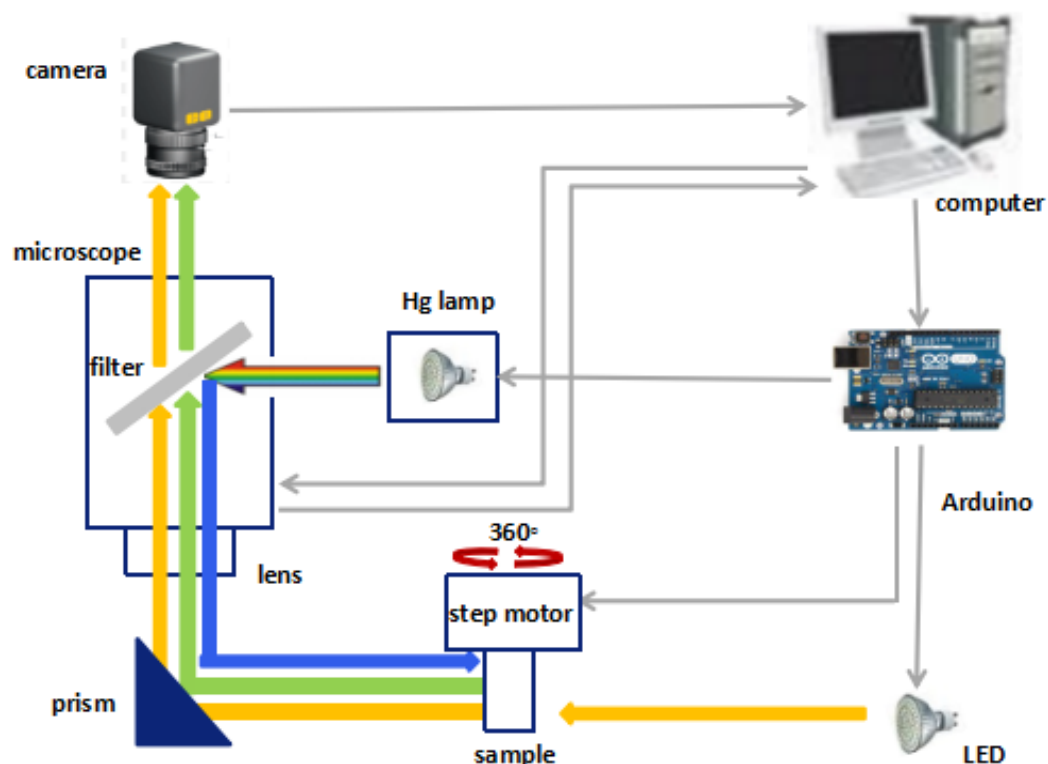
Figure 1.3. The diagram of the homemade OPT imaging system. The optical path of the bright-field channel is illustrated in yellow. The fluorescence optical path from Hg lamp goes through the filter block producing the required excitation wavelength (in blue). The emission wavelength (in green) is produced when the excitation light is excited by fluorescence protein such as GFP.

The details of the OPT imaging system are explained in Figure 1.4. As follows: (A) presents the overall view of the imaging units which consist of control unit (blue line), light path unit (purple line) and sample unit (red line). The control unit includes microcontroller Arduino and manual controller that are described in (B). The manual controller can be used for manual magnification adjustment by rolling zoom wheel. The focus wheel is used for focusing at a specific magnification. The filter change and shutter are combined to determine and change the filter for working in fluorescence mode. Set button stores the current positions of magnification/focus/filter changer/double iris diaphragm for five combinations. (C) and (D) elaborate the sample unit in which the sample is mounted and imaged. The sample, e.g. zebrafish, is embedded in agarose prior to a clearing process and after clearing glued to a cylindrical plastic stub with a metal ending. As shown in (C) the metal ending can be mounted to a magnet with a stepper motor, through a full revolution of the sample over 360°. Taking into account the refraction of light, the specimen is located in a clearing solution inside a cuvet which has the same refractive index as the sample after clearing. When the specimen is mounted to the stub its position can be adjusted by using the position bar. The sample unit is contained in a black casing to block off ambient light. To further avoid ambient light in fluorescence mode, a plastic shield is used.
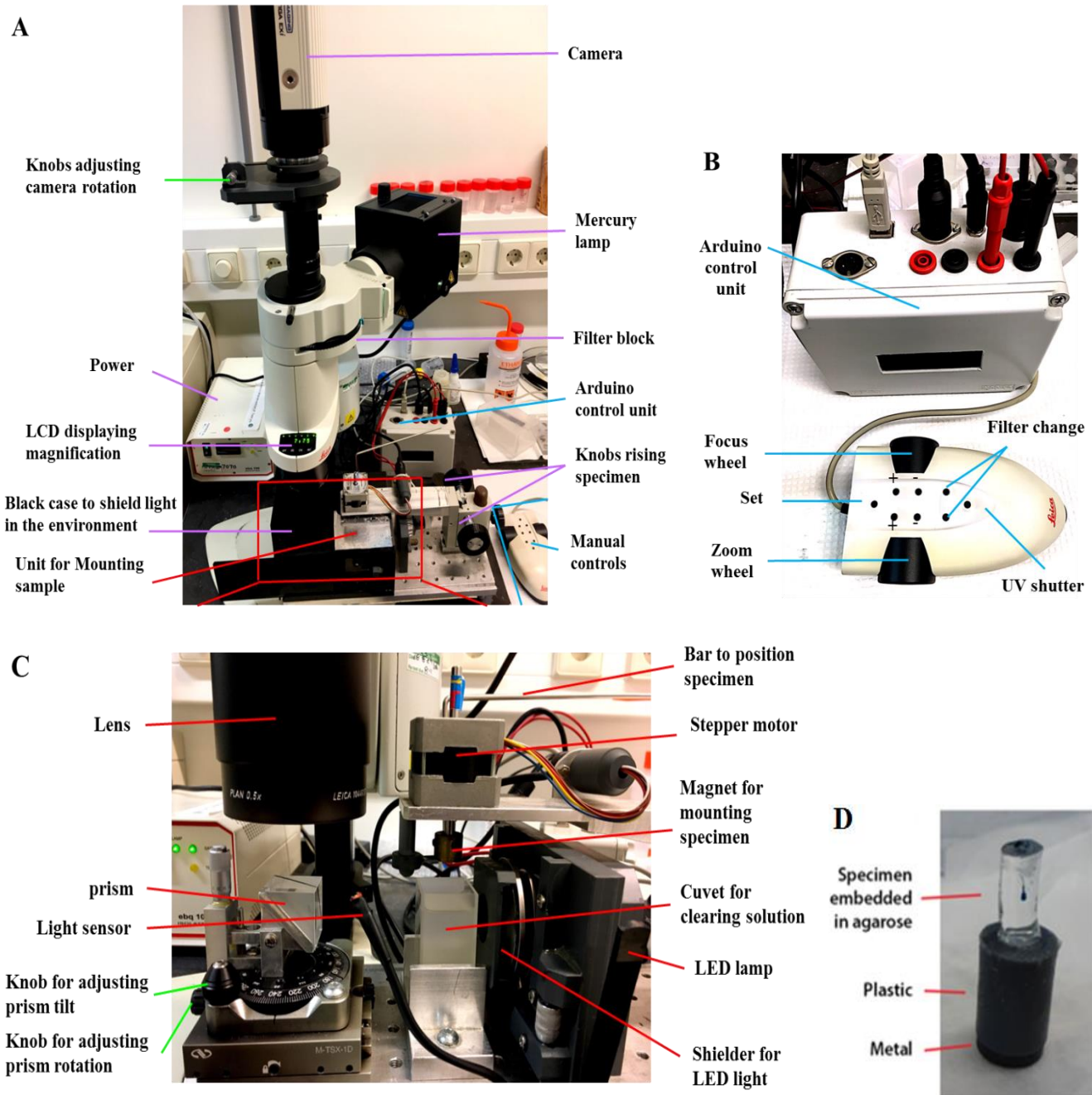
Figure 1.4. Explanation of experimental setup for the OPT imaging system. (A) The whole view of the imaging system excluding computer. (B) Unit of microcontroller chip (Arduino) and manual control. (C) Unit of imaging environment in which the specimen is located. (D) Unit for mounting specimen.

1.2.3 OPT imaging software

The graphical user interface (GUI) of the OPT imaging system contains three parts, i.e. calibration, experiment settings and imaging as depicted in Figure 1.5. The calibration parameters include camera rotation, prism rotation and prism tilt. They are combined to determine the position of the specimen in the Field of View (FoV). The camera rotation
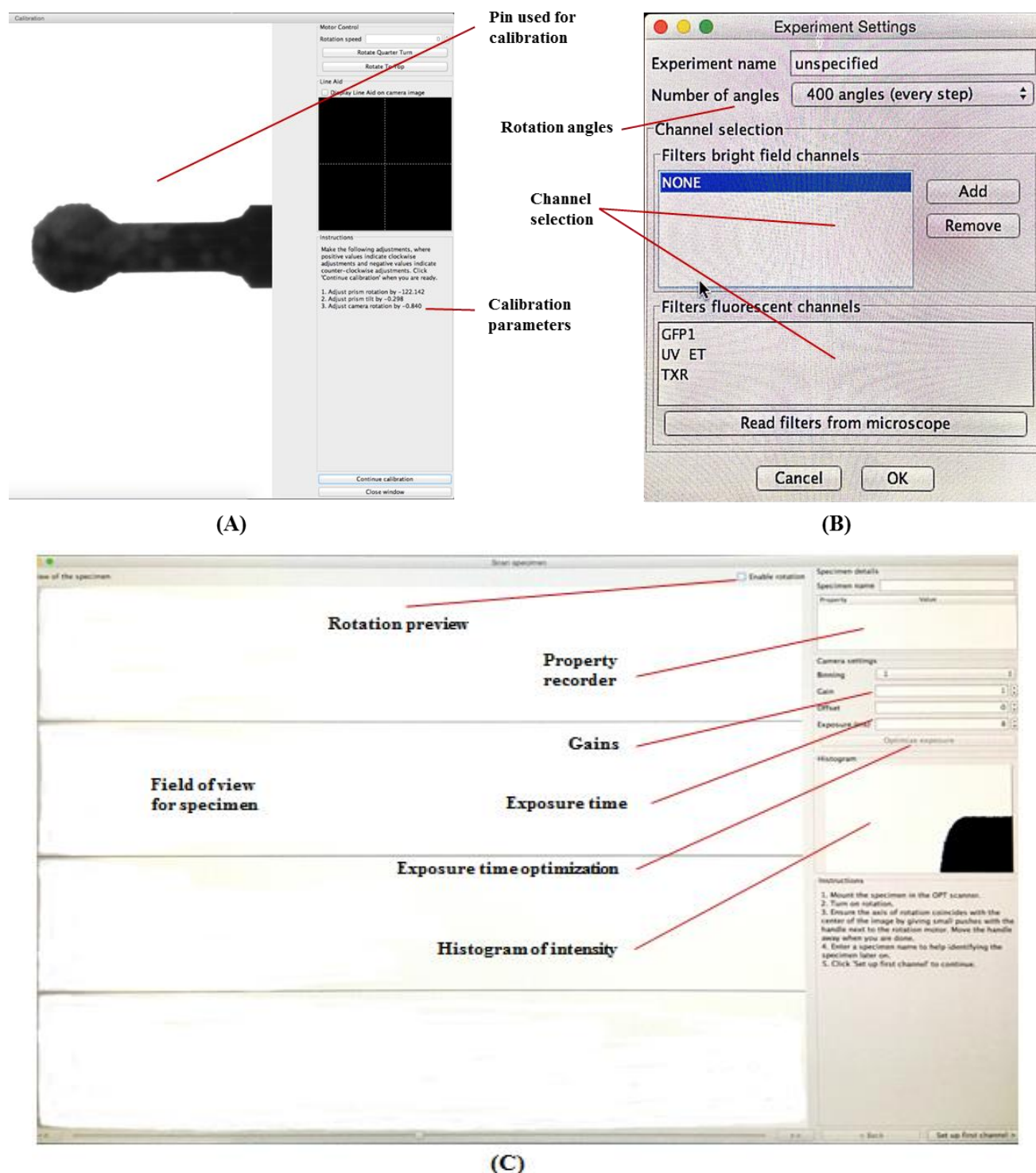
(A)

(B)

(C)

Figure 1.5. OPT imaging software. (A) The calibration user interface. (B) GUI for the experimental settings. (C) GUI for the bright-field and fluorescence imaging.

can be adjusted by the knob near the camera as annotated in Figure 1.4 (A), and the prism rotation and tilt adjustment can be completed by the knob as shown in Figure 1.4 (C). They can be adjusted separately, but the parameters calculated after each adjustment, are dependent on each other. The GUI for experimental setting specifies the number of rotation steps for a full revolution which is determined by the stepper motor. It starts with the selection for imaging mode or channel. In fluorescence mode GFP1, TXR and UV are

supported. Regarding to the imaging GUI, it first works for fluorescence imaging if both modes are selected. Each tomogram includes background correction, which means the specimen should be removed from the FoV by using two knobs as shown in Figure 1.4 (A). Figure 1.5 (C) elaborates the parameters that are required in the specimen imaging process and some useful information with respect to the image quality such as a life histogram informing on the intensity range that is employed with the current illumination settings.

1.2.4 Experimental sample preparation

Sample preparation refers to the protocols used on the specimen to assure the acquisition of useful information with OPT microscopy. It is the most time-consuming process in the OPT imaging workflow, allowing preparation of a few samples per day. Researchers, in general, need to image a lot of specimens to obtain good and statistically valid observations. We, therefore, have to considerably speed up this process.

Therefore, a protocol for efficient sample preparation including counterstaining, embedding of specimen in agarose, and optical clearing is essential to make the OPT suitable. The optimisation of the sample preparation step has been thoroughly studied [20]. This optimisation is out of the scope of our research but it significantly contributes to the quality of our image acquisition and data. Counterstaining (toluidine blue), cylindrical agarose and clearing agents (benzyl alcohol: benzyl benzoate, BABB) are mostly used for sample preparation of samples presented in this thesis.

1.3 Computational approaches of OPT imaging

From proper OPT sample preparation and imaging, we acquire the tomogram data that is, in fact, a collection of axial 2D images. For further processing and visualization we need to have the data on a regular 3D grid. Therefore computational approaches are required. These computational approaches cover 3D reconstruction, 3D segmentation, optimisation of iterative reconstruction based on segmentation performance and fluorescence quantification. For this thesis our main sample will be zebrafish.

1.3.1 3D reconstruction

The process of going from a tomogram to a 3D image defined on a regular rectangular grid is referred to as 3D reconstruction. There is no standardized manner of specimen mounting and nor do we have full control over the experimental environment; therefore a framework is needed including both fast reconstruction and accurate reconstruction to comply for different requirements. The fast reconstruction provides an efficient solution for specimens with dispersed signals, while the accurate reconstruction produces a more precise reconstruction with lesser artefacts at the expense of computation time. Fast reconstruction solves the reconstruction problem but fails to reduce artefacts. In tomography, a known category is the streak artefacts that due to local intensity loss of the

beam as a result of dense materials such are metal components. If the fast reconstruction is satisfactory, the reconstruction framework is completed. If accuracy is required and streak artefact need be removed, iterative reconstruction must be considered. Our workflow for 3D reconstruction is illustrated in Figure 1.6, with the top and bottom of the diagram showing the two different reconstruction methods. Optimisation in iterative reconstruction including initialization and iterative step, and GPU-based implementation will be explored in the research presented in this thesis, and upon evaluation, integrated in our reconstruction framework.
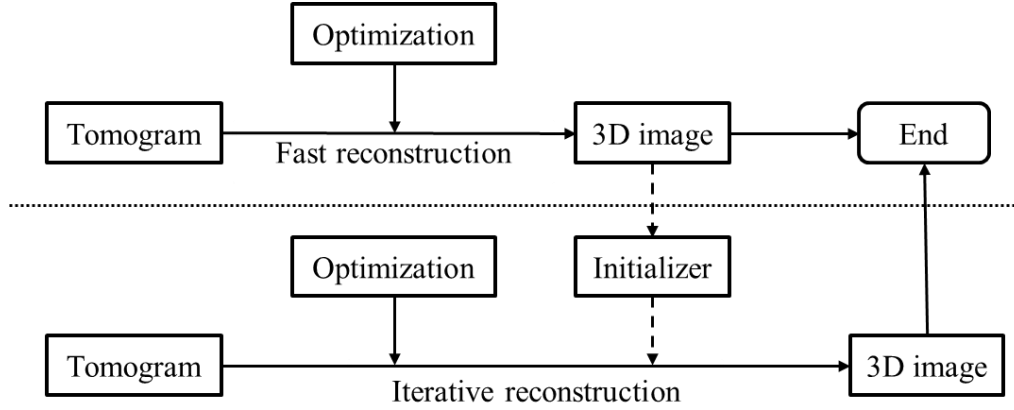

Figure 1.6. The scope of reconstruction and optimisation for OPT 3D imaging.

1) *Fast reconstruction and optimisation*

For fast reconstruction a framework is set up that takes into account, reconstruction, artefact reduction, 3D deconvolution and parallelization implementation.

The Radon transform [21] is widely applied to tomography which is produced from the projection associated with cross-sectional scans of an object, we first explore the applicability of Radon transform to our OPT imaging. The Radon transform represents, de facto, the projection data obtained as the scan from the OPT and the output is the tomogram. The inverse Radon Transform can be used to reconstruct to the initial object. The process of reconstruction with inverse Radon Transform is called back projection. The most frequently applied reconstruction algorithm for back projection is known as Filtered Back Projection (FBP) by Nygren and Anders [13]. In our fast reconstruction framework FBP will employed because of its wide applicability and efficiency.

In a previous study [22], it has been acknowledged that artefacts occurring in 3D images in OPT imaging systems are mainly introduced through two reasons. One is from the imaging setup such as non-uniform illumination, signal decay and CCD imperfection. Another sort of artefacts comes from the computational process including the centre of rotation (CoR) misalignment and limitations in the number of tomographic images that are available for the reconstruction algorithm. The artefacts from the second group, however, are more noticeable and salient; these will be studied in the following sections.

Limited by the diffraction of light in the optical imaging system, the images are unavoidably blurred in imaging process. Unlike a confocal imaging system, in tomographic images this imperfection cannot be deblurred directly from a systematic point spread function (PSF). An OPT imaging system has variant PSFs for points that are located within different distances to focal plane. How we can model the variant PSFs and take them into account in 3D image for deblur is one of our research topics of interest for optimisation in fast reconstruction.

The core for fast reconstruction is to apply parallel and distributed computing. The parallelization can efficiently decrease the computing time of the reconstruction process. We accomplish this by distributing all the slices to different processors of a computer cluster, ensuring that the 3D data is processed in a parallel manner.

2) *Iterative reconstruction and optimisation*

Iterative reconstruction refers to iterative algorithms used to reconstruct 2D or 3D images from tomographic imaging techniques such as CT and OPT. Iterative reconstruction was developed for CT imaging in order to improve the noise profiles and suppress streak artefacts that commonly show up with FBP. These algorithms are also considered superior when there is a lack of uniform angular projections or when projections are sparse. There is a large variety of iterative reconstruction algorithms, but they all have in common that it starts with an assumed initial image, computes projections from the image via a project function and updates the image according to the difference between calculated and actual projections. According to the updating strategy for the image, iterative algorithms can be categorized into four different approaches, i.e. algebraic reconstruction technique (ART) [23], iterative sparse asymptotic minimum variance (SAMV) [24], statistical reconstruction [25] and learned iterative reconstruction [26], [27]. Among all categories, statistical reconstruction and learned iterative reconstruction show relatively better performance with respect to a combination of effectiveness and robustness.

In general, iterative reconstruction can lead to a more accurate reconstruction compared to FBP. However, a large number of iterations may be required to generate an acceptable reconstruction and each of the iteration may take about the same amount of time as one FBP reconstruction does. Thus, to some extent the effectiveness of iterative reconstruction is achieved at the expense of huge computation time. One approach to reduce the number of iterations is to organize the projection data into a series of ordered subsets of evenly spaced projections and update the current estimate of the object after each subset rather than after the complete set of projections. The most commonly used algorithm that employs the subset strategy is referred to as ordered subset expectation maximization (OSEM) [28]. It improves the efficiency of iterative reconstruction with respect to computation time.

Iterative reconstruction methods have superior performance which shows by resistance to noise and streak artefacts in CT reconstruction. These algorithms, therefore are

supposed to have promising results on our OPT reconstruction where the streak artefacts are limiting the results. There are two sources for the streak artefacts with FBP reconstruction in our OPT imaging system. One is the relative lack of projections compared to perfect reconstruction without streak artefacts. This means that 400 samples over a full revolution are still not enough for FBP reconstruction in OPT because it has stronger light attenuation, comparing to CT. Another source for streak artefacts with FBP normally exists in emission OPT when the fluorescence signal is relatively small and highly concentrated, which is similar to the artefacts produced by metal components in the specimen with FBP in CT. With the aim to eliminate the streak artefacts in OPT, we will implement one of the iterative reconstruction algorithms, i.e. statistical reconstruction, for our data and optimize the results based on parameters required. Notably, there are two customary parameters to optimize. One is the initial image, in this thesis defined as initialization. It can be either none (meaning zero) or the result of fast reconstruction in our workflow (cf. dashes in Figure 1.6). The other one is the number of iteration steps for deciding the endpoint of iterative reconstruction. The impact of different parameters on reconstruction will be studied in Chapter 4.

In terms of evaluation, reconstruction, as a typical inverse problem, is characterized by the lack of benchmarks for a real imaging data. Researchers often measure the reconstruction performance by qualitatively comparing the results from different reconstruction approaches. Specifically, the qualitative measurement could either be less noises and artefacts or better image quality in terms of sharpness. With a lack of quantitative measurements for reconstruction performance, we take a first step to explore the possibility of transferring the problem of reconstruction evaluation to the segmentation evaluation. This evaluation is particularly applied to optimize the parameters for iterative reconstruction. We assume that in iterative reconstruction, reconstructions of the type of same data (e.g. zebrafish) from different parameters provide different inputs for segmentation, thus resulting in different segmentation performance for the resulting model, e.g. zebrafish. The reason why segmentation evaluation is employed as a reference for the optimisation of iterative reconstruction is that we need a good reconstruction of the specimen for a segmentation model and the segmentation performance can give us an intuitive and quantitative feedback about how good the reconstruction is. This framework works under the assumption that the same segmentation model is used. In terms of parameters in iterative reconstruction, there are several ones required but number of iterations and initialization are seen as the most customary ones. Theoretically, by applying this alternative reconstruction measurement, i.e. the segmentation performance, to the parameter optimisation of the iterative reconstruction algorithm, a more accurate reconstruction will be achieved.

1.3.2 3D segmentation of OPT reconstructions with applications to zebrafish

The OPT is particularly useful for imaging of specimen/objects in the *mm* range; so, zebrafish is a specimen typically suitable for this type of imaging. The zebrafish model

system is very popular in bio-medical research. Zebrafish can be easily embedded in large scale projects as sufficient amounts of samples can be made available. In experimental setup we are interested in the phenotype and the gene expression of the phenotype in a zebrafish sample. Measurements in zebrafish OPT reconstructions require a clean image; noise and debris should be avoided but in the practice of the imaging this is difficult to achieve. Therefore, a segmentation of the specimen is required. An OPT image can contain multiple channels. The bright-field channel typically provides the possibility for generating a whole-mount mask of the zebrafish, or any specimen in general. Noises, debris in the image and transparency of the zebrafish complicate segmentation. These facts limit the success of conventional segmentation algorithms, i.e. adaptive thresholding, mean shift to name a few. In the application of segmentation methods on zebrafish, we observe inaccurate body boundaries and the fainter transparent parts make a distinction between the foreground and the background difficult.

In order to obtain reasonably good segmentation results of zebrafish, a more advanced and intelligent segmentation approach is required. We therefore employ machine learning strategies and, for our studies, a supervised segmentation framework is presented as illustrated in Figure 1.7. The application of supervised machine learning requires a training process from examples and prior to the training procedure images of different specimens are reconstructed and labelled. Because of the information redundancy among adjacent slices in a 3D image, the training data is manually labelled in equidistant intervals. We will investigate the use of a convolutional neural network (CNN) for the training process.
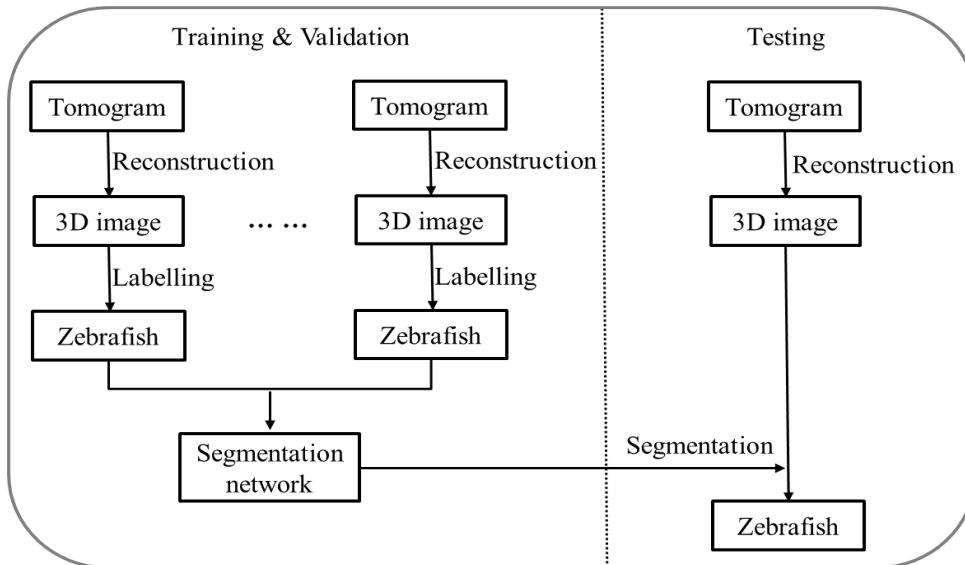
Figure 1.7. The diagram of training a zebrafish model for segmentation. The images used for training segmentation network and testing are from bright-field channel.

The labelling of all slices in the 3D image for training segmentation network is optional; if necessary, it can be obtained by either using interpolation technique or predicting from the segmentation network, such as U-net convolutional networks [29]. We investigate how

such network for 3D image segmentation could be trained either on parts of the 3D image or on the whole 3D image. A typical network that has been successfully employed for segmentation in bio-medical research is the U-net convolutional neural network [29]. The differences between training on manually labelled slices or whole 3D images are the training time and accuracy; this is extensively studied in Chapter 5. Previous results from U-net convolutional neural network have shown its usefulness in bio-medical image segmentation [30]. For training the 3D segmentation network, both 2D U-net and 3D U-net convolutional networks will be employed. The differences in performance on the data between the two networks will be explored. With the trained zebrafish segmentation network, any 3D bright-field OPT image can be semantically segmented as zebrafish or none-zebrafish. Masking the zebrafish in 3D with the corresponding 3D fluorescence channel image accomplishes general fluorescence quantification, providing valuable information for bio-medical research.

1.3.3 Quantification of volumetric fluorescence in zebrafish

We consider zebrafish as a prototypical example for OPT imaging in which we both use the bright-field as well as the fluorescent channels. The rapid development of fluorescent microscope imaging technologies in the past years, enables high-throughput 2D fluorescent imaging platforms now in widely use on both gene expression and proteome scale [31]. High data volumes for protein and/or gene expression benefit the statistical analysis. This is typically the case for such zebrafish. The 2D quantification of the fluorescence provides a relatively rough measurement for analysis. It fails to reconstruct the real, particularly spatial, distribution of fluorescence, thereby losing much useful information.

Therefore, 3D fluorescent imaging techniques, such as CLSM, OPT and MicroCT, play a significant role in obtaining insights in 3D quantification of fluorescence so that real and relatively accurate protein and/or gene expression can be computed. Due to the large amount of data in 3D imaging, high-throughput scale is currently limited by the computing and memory power. To some extent, throughput in 3D imaging and quantification is possible under the condition of efficient sample preparation and reconstruction.

In general, a correct and accurate 3D fluorescent quantification largely depends on sample preparation, reconstruction performance and image processing i.e. segmentation. The protocol of sample preparation varies depending on different imaging techniques but the common demand for a good sample preparation is supposed to suppress noise and highlight fluorescence as much as possible. In this case, prior knowledge is typically required to distinguish between the noise and the fluorescence signal we are interested in. The segmentation process supports in understanding the information about what is useful or significant to the quantification. In order to achieve reliable 3D quantification of fluorescence in a smaller data volume, segmentation can be manually accomplished using prior knowledge. This approach is however, not feasible for larger scale of data, for

instance some-throughput imaging of zebrafish in our OPT system. This is a motivation for us to investigate the utility of a trained 3D zebrafish reference structure for the 3D quantification of fluorescence in zebrafish. In this thesis we present the framework of 3D quantification of fluorescence in zebrafish, but it can be easily transferred to other applications such as 3D quantification of fluorescence in zebrafish/mice brain, liver, kidney, etc.

1.4 Research questions and perspectives

RQ1: To what extent is it possible to increase the processing speed of OPT imaging and reconstruction in an integrated manner?

The 3D reconstruction as a post-imaging process, is therefore separated from OPT imaging system. This separation can be physical, i.e. computations on different computers. The time of one reconstruction varies from minutes to hours depending on the reconstruction algorithm and computation resources. This means that in a worse case it may take multiple hours to generate one 3D OPT image. With the further development of data science in bio-medical research the availability of data becomes increasingly important. To provide more bio-medical data, i.e. 3D OPT images in our case, it is of great importance to decrease the imaging time and increase the efficiency of 3D imaging process. Therefore, we investigate integrating the imaging and reconstruction as a whole and implementing the reconstruction in a parallel fashion. With respect to the reconstruction algorithm, the fast and efficient reconstruction, i.e. FBP is first taken into account. What interests us is how much improvement can be achieved regarding the imaging time and efficiency of computation.

RQ2: To what extent is it possible to reduce the artefacts of 3D image introduced during reconstruction process by misalignment of CoR?

According to Singh *et al.* [19], there are several types of artefacts in OPT reconstruction. One of them is the edge blur artefacts introduced by CoR misalignment. It means that the rotation centre of the imaging system is shifted off the centre of FoV. This shift inevitably exists unless a very accurate mechanical calibration is included. This mechanical calibration process is typically time consuming and requires a lot of operator interaction. Instead of eliminating the shift in the pre-imaging calibration process, we are interested in correcting it in the post-imaging process before reconstruction.

The aforementioned pre-imaging shift will introduce a problem that the CoR is not accordance with the image centre. This means that the reconstructed slices will consequently be corrupted by the edge blur artefacts after application of the reconstruction algorithm. The motivation for this research is to detect and correct the CoR shift in tomogram and further eliminate the corresponding artefacts in the reconstruction process. To this end, a fast and accurate CoR correction algorithm is

needed. How much improvement will be achieved should be qualitatively and quantitatively analysed and explored.

RQ3: Can the PSF of the OPT imaging system can be modelled and applied for deblurring of an OPT reconstruction?

In general, an imaging system is described by the ability of giving a response to a point light source or object, commonly referred to as the point spread function (PSF). A more general term for the PSF is a system's impulse response, being the impulse response of a focused optical system. For OPT imaging and reconstruction, the DoF is expected to be large enough to contain the specimen to be visualized as much as possible. According to the previous studies [32], [33], however, large DoF subsequently results in low in-focus image quality. The trade-off between DoF and image quality should be considered when selecting a lens for the OPT imaging system. A lens with small NA will produce large DoF, allowing imaging of larger specimens but it will result in a relatively low-quality image. Contrarily, a lens with large NA yields relatively high-quality images but cannot image the whole specimen with respect to its size.

One typical way to improve the image quality of 2D imaging system to the best possible resolution, is to apply deconvolution to the images, using a constant theoretical or experimental PSF as the kernel for deconvolution. However, this approach is not strictly suitable for OPT images. Because first, the tomogram normally integrates the information of a specimen at different depths within a wide field, not a fixed depth on the focal plane. Second, the imaging PSF within the field varies at different depths along the optical axis. This means that different PSF is produced when locating the point source at different depths. While the conventional 2D PSF and deconvolution are not feasible for OPT imaging system, we are interested in how a variable PSF could be modelled in OPT imaging system and how much image quality improvement can be achieved when using it in deconvolution of the 3D image.

RQ4: Can the iterative reconstruction eliminate the streak artefacts produced in the fast reconstruction?

With the fast FBP reconstruction, a 3D image can be obtained. For specimens with sparse and large-area signals, it produces satisfactory reconstruction when CoR misalignment is solved. However, when imaging specimens with a dense and concentrated signal such as concentrated fluorescent GFP signal, the FBP algorithm will produce streak artefacts because of the sample limitation. There are several methods such as linear interpolation (LI) and the state-of-the-art normalized metal artefacts reduction (NMAR) to decrease the streak artefacts in CT in an FBP framework [30], which may be useful for OPT 3D reconstruction. But these approaches seem to reduce the artefacts in the reconstruction but do not eliminate the artefacts. In order to eliminate the streak artefacts, iterative reconstruction has proven to be promising in CT reconstruction [34]–[36]. Inspired by the

results in CT imaging, we are interested in exploring if iterative reconstruction can help to eliminate the streak artefacts in OPT reconstruction and how it works. In our work both reconstruction frameworks are available, depending on application of what a certain reconstruction algorithm is chosen.

RQ5: How and to what extent the initialization and the number of iteration steps influence the results in iterative reconstruction?

Iterative reconstruction can eliminate the streak artefacts, thus it could be used as a prospective method to produce an accurate OPT reconstruction at the expense of time compared to fast reconstruction such as FBP. Sometimes these accurate reconstructions are essential. Considering the non-deterministic process of iterative reconstruction, the results are influenced by the parameters of algorithm. In this research we investigate the most customary parameters, i.e. iteration steps and initialization. To explore the effect of iteration steps on reconstruction, we reconstruct the tomogram with different iteration steps. With respect to initialization, we compare the results produced with a setup of no initialization to those with an initial reconstruction that are obtained by fast reconstruction as described in Chapter 2.

With the different reconstructions to compare, an evaluation criterion is required. In bio-medical research it is not always possible to construct a benchmark for both 2D and 3D imaging because of different specimens and experimental setups. For instance, to assess the various reconstructions in our study, there is no theoretically ideal reconstruction that can typically be used as benchmark for evaluation. Therefore, instead of assessing the reconstructions directly, we investigate a framework to assess the segmentation results of the reconstruction indirectly. The benchmarks of the segmentation are easier to obtain by labelling the data. The evaluation of reconstructions of different experimental setups is transferred to the evaluation of the corresponding segmentation results.

RQ6: Is it possible to "learn" a 3D reference structure of zebrafish for 3D fluorescence quantification in zebrafish?

Zebrafish are valuable for studies of a multitude of diseases including cancer, heart disease, obesity, muscular dystrophy and narcolepsy. They are easy to maintain and cost-effective. One key feature is that, following fertilization, zebrafish embryos are transparent and their rapid embryonic development can be observed. Another important reason is that zebrafish as a vertebrate is similar to human, making it a suitable model for many human diseases [37].

Because of the imperfections in sample preparation and experimental imaging environment, a specific fluorescence may exist around a specimen in the background. It is therefore required to segment the specimen from the background. For our study in zebrafish, segmenting and recognizing zebrafish volume from background are of great

importance for fluorescence quantification. For the volume, the fluorescent signal must be counted and quantified just there where zebrafish sample is, otherwise it should not be considered. The segmentation of zebrafish also plays an important role in reference structure detection for high-throughput quantification where relative measurement is considered. This will be elaborated in Chapter 5. To train and learn a theoretically robust segmentation model for 3D reference structure detection, a large number of zebrafish are acquired at different stages and in different experimental environments. By using the trained segmentation model as a classifier, the 3D image reconstructed from a specimen can be identified as reference structure or not. The 3D fluorescent signal, e.g. tumour in Chapter 5, can be quantified and normalized referring to the reference structure that is identified. Compared to 2D, such accurate 3D fluorescence quantification helps to improve the research results in for instance drug discovery.

RQ7: How much 3D information can be achieved and identified from bright-field images of zebrafish and to what extent can the identification of parts be automated?

In the OPT imaging system, bright-field image contains some extent of structures or context information of zebrafish. It also represents the minimum of details of zebrafish structure without any staining techniques. Some structures, e.g. eyes play an important role in accurate positioning analysis of protein and gene expression patterns. In order to explore how much structural detail within zebrafish can be identified for such analysis, we manually label the 3D image of zebrafish in two different very distinct developmental stages, i.e. 5 *dpf* and 25 *dpf*. The results are visualized and the two developmental stages are qualitatively compared to provide an intuitive clue for phenotype analysis of these structures. Furthermore, in view of the trends in order to study the possibility of trending high-throughput analysis in 3D, we are curious about how automated 3D structure detection algorithm can facilitate and accelerate the manual labelling process, as well as how much accuracy can be achieved by using the automated detection. If the accuracy is not satisfactory, how can we propose the possible solutions to improve it for further advanced analysis?

1.5 Thesis structure

This thesis is structured along the research questions presented in the previous paragraph.

In **Chapter 1** "**Introduction**" a brief introduction on the 3D imaging, reconstruction framework in OPT microscopy is given. Besides that, our scope for reconstruction optimisation, 3D segmentation and its application value are elaborated. To clarify these research topics, seven research questions are proposed.

Chapter 2 "**Fast Post-processing Pipeline for Optical Projection Tomography**" presents a fast reconstruction framework to improve the effectiveness and efficiency of OPT 3D reconstruction. It is implemented in a parallel manner and the experiments show

that the average run time for each tomogram is less than 5 minutes in our current setup. In the framework a novel CoR correction method based on interest point detection in sinogram, is proposed by taking the principle of OPT imaging into account. To quantify and compare the reconstructed results of different CoR correction approaches the coefficient of variation (CV) instead of the variance is employed.

Chapter 3 "**Deblurring Images from 3D Optical Projection Tomography Using Point Spread Function Modelling**" focuses on the deblurring of the reconstructed 3D image. When imaging large specimens with OPT imaging system, a large depth of field is required. This normally results in blur, i.e. compromises the image quality. Yet, it is important to obtain the best possible quality 3D image from the OPT, thus deblurring the image is vital. To this end we first model the PSF along optical axis at different depths. Meanwhile the magnification is taken into account in the PSF modelling. Subsequently, deconvolution in the coronal plane based on the modelled PSF is implemented to accomplish deblurring of the OPT image. Experiments with the proposed approach based on 25 3D images including 4 categories of specimens, indicate the effectiveness of quality improvement assessed by image blur measures in both spatial and frequency domain.

Chapter 4 "**Segmentation-driven Optimisation for Iterative Reconstruction in Optical Projection Tomography: An Exploration**" introduces GPU based iterative reconstruction aiming for the best possible, reconstructed from an OPT tomogram. Here possible streak artefacts produced by FBP reconstruction should be eliminated. The reconstruction performance with different initializations and iteration steps is evaluated indirectly based on the segmentation results of the reconstruction, instead of the reconstruction itself. Aiming at producing good segmentation results, a deep learning model is employed. The iteration step and initialization of the iterative reconstruction are considered optimal when evaluation measurement reaches a maximum. The model is trained and tested on three 25 *dpf* 3D zebrafish image from bright-field tomograms.

Chapter 5 "**Automated Detection of Reference Structures for Fluorescent Signals in Zebrafish with a Case Study in Tumour Quantification**" aims at automatically detecting the reference structure to relatively quantify the 3D fluorescence within a zebrafish. We will build and train a segmentation model to automatically detect the zebrafish *Body* and *Eye* reference structure in two different data spaces (i.e. 2D slice and 3D volume, c.f. Chapter 5) and optimize the segmentation model individually. Subsequently, the segmentation performances are compared and evaluated. The approach with the best performance will be considered for the automated detection of reference structure for tumour quantification as a case study for drug research.

Chapter 6 "**Exploration of 3D Structure Annotation and Visualization of Zebrafish Reconstructions from Optical Projection Tomography Imaging**" explores the

possibility of volume region annotation in OPT imaging. The aim of this chapter is to, first give an idea of how much volume region information can be acquired and reconstructed using our OPT imaging system on whole-mount specimen. Second, it explores the possibility of automated annotation of volume region within zebrafish, which are potentially important for the high-throughput research at level of organ systems. In the first case, up to 9 parts or volume regions of a 25 *dpf* zebrafish can be segmented and visualized using OPT. Nevertheless, automated segmentation of such volume regions has proven to be challenging and is still limited by data size and segmentation algorithm.

Chapter 7 "**Conclusions & Discussion**" summarizes our contribution for 3D OPT imaging, reconstruction, structure detection and visualization framework and states some drawbacks of the framework. Future improvements of our framework are discussed guaranteeing the integrity of the framework.